

Observation of Centrifugally Driven Interchange Instabilities in a Plasma Confined by a Magnetic Dipole

B. Levitt,* D. Maslovsky, and M. E. Mauel

Department of Applied Physics and Applied Mathematics Columbia University, New York, New York 10027, USA

(Received 16 October 2004; published 4 May 2005)

Centrifugally driven interchange instabilities are observed in a laboratory plasma confined by a dipole magnetic field. The instabilities appear when an equatorial mesh is biased to drive a radial current that causes rapid axisymmetric plasma rotation. The observed instabilities are quasicohherent in the laboratory frame of reference; they have global radial mode structures and low azimuthal mode numbers, and they are modified by the presence of energetic, magnetically confined electrons. Results from a self-consistent nonlinear simulation reproduce the measured mode structures.

DOI: 10.1103/PhysRevLett.94.175002

PACS numbers: 52.35.Mw, 52.72.+v, 94.30.Hn

Because of its relationship to the gravitational Rayleigh-Taylor instability found in stratified fluids, the interchange instability in magnetized plasma is among the best known in plasma physics. Interchange instabilities occur in a variety of natural and artificial situations, including the gravitational Rayleigh-Taylor instability found in the *F*-layer of the ionosphere [1] and the pressure-driven interchange instability found in magnetic confinement configurations [2]. Since the interchange instability mixes plasma while minimizing changes in the magnetic field, its nonlinear evolution can lead to beautiful and complex transport mechanisms. For example, in steady current-free plasma discharges created within a magnetic trap with purely toroidal curvature, the interchange mode evolves into a rotating electrostatic dipole vortex [3] that transports mass, energy, and charge [4].

The centrifugally driven interchange instability plays an especially important role in the Jovian magnetosphere since interchange mixing is likely to be the mechanism for outward transport of ionized matter emanating from Io, an inner moon [5,6]. Satellite measurements form a consistent estimate of the average mass outflow velocity [7], and small “empty” flux tubes have been detected [8,9] that may represent the buoyant, inward-moving return flux. Although the centrifugal interchange instability has been modeled theoretically [10–12] and computationally [13], the spatial structures [14] and particle interactions [15] of centrifugal interchange dynamics are still poorly understood.

In this Letter, we report the first laboratory observation of the centrifugally driven interchange instability in magnetized plasma. The observations were made using a laboratory terrella device, the Collisionless Terrella Experiment (CTX) [16–19], that was modified with an axisymmetric tungsten mesh placed at the equator of the dipole magnet and protruding about 1 cm into the plasma. When the mesh is negatively biased with respect to the outer vacuum vessel wall, the resulting radial current produces a rapid azimuthal plasma rotation and an outward centrifugal force on the plasma. Several movable probes

show the plasma has a nearly rigid azimuthal rotation and a steep radial density profile. Using a multiprobe correlation technique [18], the radial and azimuthal structures of the instability’s electrostatic potential fluctuations are measured and found to have long wavelengths comparable to the system size. Since the plasma contains a population of energetic, magnetically trapped electrons, the effects of collisionless, rapidly drifting particles are also studied. Both pressure-driven and centrifugal-driven interchange modes can occur during the same discharge, but they modulate each other. In rapidly rotating discharges having reduced populations of fast electrons, the dominant wavelength of the centrifugal mode becomes somewhat shorter as is consistent with theoretical and numerical models [20].

The CTX device has been described previously [16–19]. A dipole magnetic field is created by a strong, mechanically supported electromagnet positioned at the center of a large metallic ultrahigh vacuum chamber approximately 140 cm in diameter. Plasma discharges are produced with an injection of 2.45 GHz microwaves that resonate with the cyclotron frequency of electrons trapped by the dipole magnetic field. The rates of microwave heating and of energetic electron production are most intense at the radial location where the fundamental cyclotron resonance is located at the equatorial plane. As a consequence, when the background hydrogen gas pressure is properly adjusted ($\sim 10^{-4}$ Pa), a so-called “artificial radiation belt” forms, consisting of an annulus of anisotropic energetic electrons ($E_{\perp} \sim 1\text{--}10$ keV $\gg E_{\parallel}$). By increasing the gas pressure, the plasma density increases while the density of energetic electrons decreases. Measurements at many regions in the plasma are made by movable probes [18].

When the newly-installed tungsten mesh is biased negatively, a net radial current is induced, and the equilibrium electrostatic potential decreases in a manner similar to the recent report by Saitoh and co-workers [21]. With positive bias, no equilibrium changes were observed as was also reported by Saitoh. Defining the magnetic field by the azimuthal angle, magnetic flux, and scalar potential, $\mathbf{B} = \nabla\phi \times \nabla\psi = \nabla\chi$, the plasma rotation induced by the ra-

dial electric field is $\omega_E(\psi) = -\partial\Phi/\partial\psi$. Figure 1 shows the measured equilibrium potential profile for a mesh bias of -500 V. The various probe measurements are mapped to magnetic field line coordinates, $(L, \phi, s) \rightarrow (M_0/\psi, \phi, \int d\chi/B)$. When plotted as a function of the equatorial radius, the potential scales as $\Phi \propto 1/L$. This implies rigid plasma rotation about the dipole axis. For the conditions in Fig. 1, $\omega_E/2\pi \approx 19$ kHz and is apparently constant (since $\psi = M_0/L$, with $M_0 = 1.7 \times 10^{-3}$ T m³ being the full-current dipole moment for CTX). The radial current is proportional to the plasma rotation rate and a weighted, field line integrated Pedersen conductivity, $I = 8\pi M_0 \Sigma_p \partial\Phi/\partial\psi$, where $\Sigma_p \equiv \int d\chi \sigma_p |\nabla\psi|^2/B^2 / \int d\chi |\nabla\psi|^2/B^2$. Since ω_E appears constant, so is Σ_p . For this to happen, the local cross-field conductivity, σ_p , must have a form related to the magnetic geometry. We find the overall level of the radial current, ~ 2 mA, is consistent with a conductivity due to ion-neutral collisions, $\sigma_p \approx nM_i\nu_{in}/B^2$, with measurements of the plasma density, n at the edge, and the measured neutral pressure. While the variation of the ion-neutral collision frequency within the plasma is not known, if it were constant $\nu_{in} \sim 500$ s⁻¹, then rigid rotation occurs when the equatorial plasma density scales with the radius as $n \propto 1/L^6$. Measurements of the ion saturation current at the outer regions of the plasma, shown in Fig. 1(b), are not too different from this profile. These measurements are also steeper than the local criterion for marginal stability, $n \propto 1/L^4$. For the experiments reported here, the power required to maintain plasma rotation was 1–2 W.

When the tungsten mesh is biased sufficiently negative, electrostatic fluctuations appear that we identify as the centrifugal interchange instability. No instabilities are found with positive bias, consistent with the absence of an enhanced radial electric field. The fluctuations are mea-

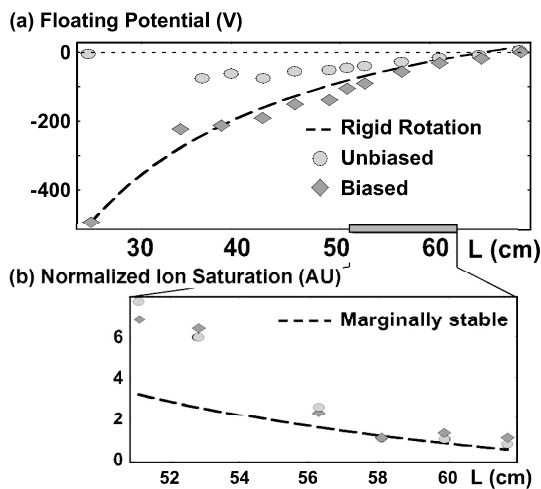


FIG. 1. Equilibrium profiles of the (a) floating potential and (b) ion saturation current measured with and without external bias. In (b), the marginally stable profile for the centrifugal mode, $n \propto 1/L^4$, is superimposed.

sured in the same way that was used to identify interchange instabilities driven by energetic electron pressure [18]. We find the rotationally driven fluctuations have very different characteristics, and they are easily distinguished from the instability driven by energetic electrons. The frequency is near (but slightly above) the plasma rotation rate, ω_E (instead of the fast magnetic drift frequency of the energetic electrons, $\omega_{dh}/2\pi > 0.1$ MHz); the amplitude of the fluctuations are 1–2 V (about 20–50 times smaller than the amplitude of the energetic electron interchange), and the spectrum of the saturated instability evolves slowly as the equilibrium evolves (and periodic bursting is not observed). The most intense centrifugal instabilities occur as the density of the neutral gas is adjusted higher as well as when the strength of the magnetic dipole is lowered. These adjustments reduce the pressure of energetic electrons and lead to faster rates of plasma rotation.

Figure 2 shows a short, ~ 0.12 s, interval during a discharge when the level of external mesh bias increases from -250 to -400 V. As the bias increases, the spectral characteristics and azimuthal structures of the fluctuations evolve as measured by two probes separated by $\Delta\phi = 90^\circ$. At low and moderate biases, Fig. 2(b), the fluctuations are nonsinusoidal with a dominant $m = 1$ azimuthal mode structure. As the bias level further increases, the azimuthal flow measured using a two-side probe (i.e., a “Mach probe”) shows a sharp increase and the fluctuations transition to higher frequency and have a $m = 2$ azimuthal structure, Fig. 2(c). The measured phase difference between the probes shows that the electrostatic fluctuations rotate in the same direction and near the same speed as the plasma, ω_E .

The electrostatic structure of the fluctuations is measured by performing a correlation analysis with the movable high-impedance floating potential probes [18]. The nonequilibrium potential is measured by comparing correlations at a specific frequency, ω_m , to the definition, $\tilde{\Phi}(L, \phi, s, t) \equiv \sum_m \text{Re}\{\tilde{\Phi}_m(L) \times \exp[i(m\phi + k_L L - \omega_m t)]\}$. Although the amplitude may change slowly, the radial structure of the centrifugal interchange, $\tilde{\Phi}_m(L)$, does not change significantly in time. No phase or amplitude variations were detectable between two probes located at different s on the same field line as expected for a flute mode.

Figure 3 shows the measured radial mode structure for the three lowest azimuthal modes, $m = 1, 2, 3$. The data represent the average amplitude relative to a fixed reference probe located at $L = 55$ cm computed. The radial profile of the normalized magnitude of the two-probe correlation function has a broad structure and depends weakly on the azimuthal mode number. For all three modes, the radial structure extends smoothly from the inner region, $L \sim 0.27$ m, where hot electrons are created at the microwave cyclotron resonance, out to a radius near, but just within, the outer vacuum vessel wall, $L \sim 0.67$ m. The radial phase, not shown here, has a significant $\sim \pi/2$ radial phase shift for the dominant $m = 1$ mode. This

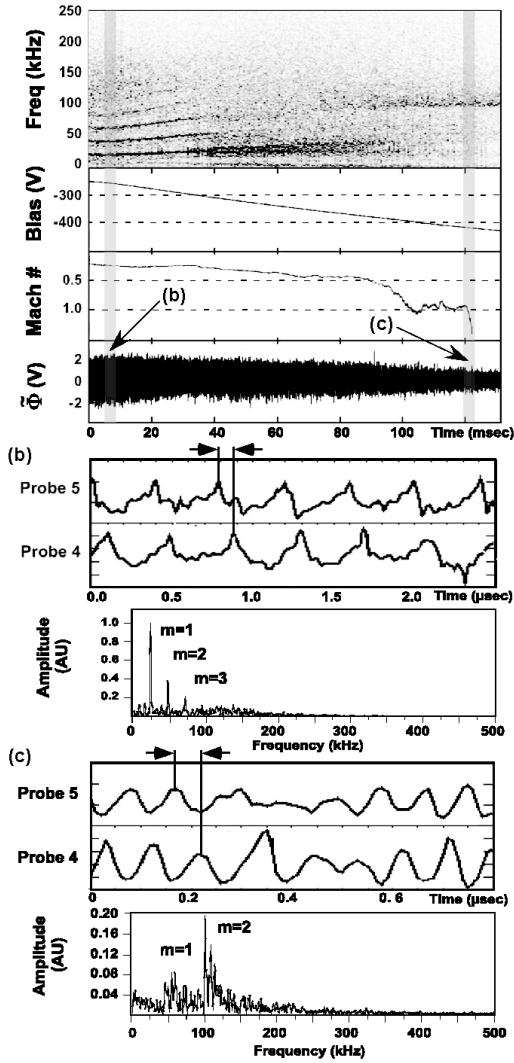


FIG. 2. Measurements of electrostatic fluctuations as mesh bias and plasma rotation increase. At moderate rotation (b), the fluctuations are nonsinusoidal but possess an $m = 1$ azimuthal structure. At stronger rotation (c), the fluctuations saturate with a continuous $m = 2$ structure.

indicates the potential fluctuations have an azimuthal “spiral” structure. For the time intervals when the correlation measurements are taken, this broad, spiral structure appears to rotate rigidly in time.

In order to interpret the observed centrifugal instability, we have modified a nonlinear, self-consistent numerical simulation [17,18]. Since the plasma undergoes rigid rotation, the modification required to model the centrifugal interchange instability is easily implemented when the evolution equations are expressed in the plasma’s rotating frame. In this frame, only the equation for cold ion dynamics changes. Using previous notation [17,18], the number of ions within a tube of unit flux, $N_i(\psi, \phi, t)$, evolves in time due to the net flux of ions caused by density-weighted, field line averaged particle drifts,

$$\frac{\partial N_i}{\partial t} + \frac{\partial}{\partial \phi} \left[cN_i \left(\omega_g(\psi) - \frac{\partial \tilde{\Phi}}{\partial \psi} - \kappa_\phi \frac{\partial \dot{\tilde{\Phi}}}{\partial \phi} \right) \right] + \frac{\partial}{\partial \psi} \left[cN_i \left(\frac{\partial \tilde{\Phi}}{\partial \phi} - \kappa_\psi \frac{\partial \dot{\tilde{\Phi}}}{\partial \psi} \right) \right] = 0, \quad (1)$$

where $\omega_g(\psi) \approx -0.58\omega_E^2/\omega_{ci}^* \propto L^3$ is the net ion drift due to the centrifugal force. The centrifugal force varies along a field line and reverses sign as the field line approaches the magnetic poles. However, these variations are irrelevant for the electrostatic interchange mode. It evolves according to the motion of plasma contained within entire flux tubes. Interchange motion in a dipole is an example of fluid dynamics in only two dimensions, (ψ, ϕ) . The Coriolis correction proportional to $\omega_E/\omega_{ci} \sim 0.03 \ll 1$ and can be ignored. The ion polarization terms are $\kappa_\phi \approx 0.66/(\omega_{ci}^*\psi)$ and $\kappa_\psi \approx 0.77\psi/\omega_{ci}^*$, where ω_{ci}^* is the ion cyclotron frequency at the equatorial plane of a field line.

Starting from a specified initial condition, the simulation explicitly solves for the time evolution of multiple, charged fluids (i.e., the ions and a collection of energetic electron populations) that are defined on a (ψ, ϕ) grid and interact nonlinearly through a perturbed electrostatic potential, $\tilde{\Phi}$. The system is entirely closed (i.e., no particles are lost or added), and $\tilde{\Phi}$ vanishes at the surfaces of the vacuum vessel and the dipole magnet. Interchange stability is determined by the rotation rate, ω_E , the fraction of energetic electrons, $\alpha(\psi)$, and the initial plasma profile, $N_i(\psi)$. Additionally, a small nonresonant dissipation is added to damp potential fluctuations. Dissipation is needed to explain the nonlinear phenomena of “frequency sweeping” that has been observed in CTX [17–19].

The initial conditions selected to model the observations reported here are similar to those reported previously [18,19] except the energetic electron pressure was reduced,

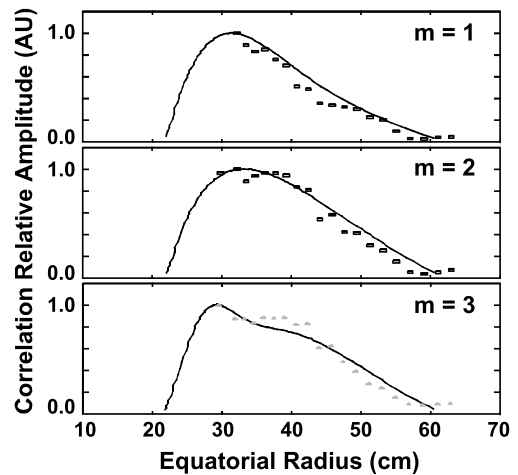


FIG. 3. Measurement of the normalized magnitude, $\tilde{\Phi}_m(R)$ of the electrostatic fluctuations measured using multiple-probe correlations. The lowest three azimuthal modes, $m = 1, 2,$ and 3 , are shown. Solid lines are simulation results.

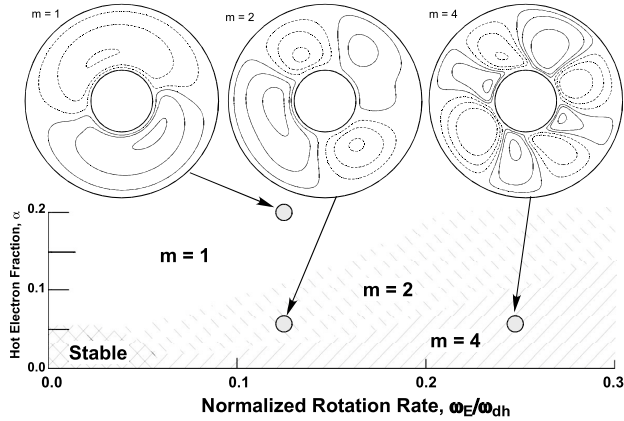


FIG. 4. Computed variation of the interchange mode structure as the fraction of energetic electrons, α , and the plasma rotation rate, ω_E , changes. Only the regimes dominated by $m = 1$ and 2 are seen experimentally.

reflecting the effects of higher neutral gas pressures and reduced dipole field. The average magnetic drift frequency of the energetic electron energy was halved, and the fraction of hot electrons, α , ranged from 5% to 20%.

As the centrifugal drive, ω_g , increased and the energetic electron fraction decreased, the nature of the interchange instability changed significantly. For $\alpha \sim 0.05$ and rapid plasma rotation, $\omega_E/\omega_{dh} > 0.2$, the most unstable interchange mode has a short wavelength, $m = 4$, and grows with nearly zero real frequency in the rotating frame. This mode represents the “ideal” rotational interchange [5] with a linear growth rate, γ , given by $\gamma^2 \approx \omega_{ci}\omega_g d(\ln N_i)/d(\ln \psi)$. As the rotational drive is reduced or when the energetic electron population increases, the azimuthal mode number, m , decreases and the interchange mode acquires a real frequency in the direction of the electron magnetic drift. A localized linear theory of the interchange mode interacting with a distribution of deeply trapped electrons shows the real frequency results from electron drift resonance [20]. When $\alpha = 0.2$ and $\omega_E/2\pi \approx 19$ kHz, the mode frequency is approximately 7 kHz in the rotating frame or 26 kHz in the laboratory frame. As α increases further, the interchange mode rotates more quickly and the fastest growing mode is dominated by $m = 1$. Figure 4 summarizes the computed interchange mode structures as a function of ω_E and α . It is noteworthy that the rate of ion circulation within the perturbed electrostatic potential is relatively slow (~ 50 Hz) compared with the rate of plasma rotation and production.

The simulation reproduces the measured radial structures of the centrifugal interchange mode. This is shown in Fig. 3 by the solid lines superimposed with the correlation measurements. We believe the remarkably good agreement is a general consequence of solutions to Poisson’s equation that take into account the dielectric properties of plasma confined by a dipole magnetic field. This was first noted for

the electron pressure-driven mode [18]. Indeed, the broad mode structures of both the fast, $\omega \sim m\omega_{dh}$, energetic electron mode and the much slower, $\omega \sim m\omega_E$ (and lower amplitude), centrifugal mode are similar. The main differences are that the centrifugal mode is broader and has a weak spiral structure, reflecting its different source of field line charging.

In summary, we report the first experimental observations of the centrifugally driven interchange mode in a magnetized plasma. The CTX plasma has a steep density profile that becomes unstable when made to rotate. The modes have a broad radial structure and have low azimuthal mode number, m . As the rate of plasma rotation increases and with reduced energetic electron fractions, the dominant mode increased from $m = 1$ to 2. A self-consistent simulation reproduces the observed mode structure. Observations of interchange-induced transport and the interaction between the centrifugal and energetic electron modes are described elsewhere [20].

*Electronic address: b1187@columbia.edu

- [1] M. C. Kelly, *The Earth’s Ionosphere* (Academic Press, New York, 1989).
- [2] G. Bateman, *MHD Instabilities* (MIT Press, Cambridge, MA 1978).
- [3] F. J. Øynes, H. L. Pécseli, and K. Rypdal, *Phys. Rev. Lett.* **75**, 81 (1995).
- [4] K. Rypdal, O. E. Garcia, and J.-V. Paulsen, *Phys. Rev. Lett.* **79** 1857 (1997).
- [5] D. B. Melrose, *Planet. Space Sci.* **15**, 381 (1967).
- [6] C. T. Russel, *Adv. Space Res.* **33**, 2004 (2004).
- [7] C. T. Russel, M. G. Kivelson, K. K. Khurana, and D. E. Huddleston, *Adv. Space Res.* **26**, 1671 (2000).
- [8] M. G. Kivelson, K. K. Khurana, C. T. Russel, and R. J. Walker, *Geophys. Res. Lett.* **24**, 2127 (1997).
- [9] R. M. Thorne *et al.*, *Geophys. Res. Lett.* **24**, 2131 (1997).
- [10] G. K. Siscoe and D. Summers, *J. Geophys. Res.* **86**, 8471 (1981).
- [11] T. W. Hill, A. J. Dessler, and L. J. Maher, *J. Geophys. Res.* **86**, 9020 (1981).
- [12] D. J. Southwood and M. G. Kivelson, *J. Geophys. Res.* **92**, 109 (1987).
- [13] Y. S. Yang *et al.*, *J. Geophys. Res.* **99**, 8755 (1994).
- [14] K. M. Ferrière, C. Zimmer, and M. Blanc, *J. Geophys. Res.* **106**, 327 (2001).
- [15] A. N. Fazakerly and D. J. Southwood, *J. Geophys. Res.* **97**, 10787 (1992).
- [16] H. P. Warren and M. E. Mael, *Phys. Rev. Lett.* **74**, 1351 (1995).
- [17] M. E. Mael, *J. Phys. IV* **7**, 307 (1997).
- [18] B. Levitt, D. Maslovsky, and M. Mael, *Phys. Plasmas* **9**, 2507 (2002).
- [19] D. Maslovsky, B. Levitt, and M. E. Mael, *Phys. Rev. Lett.* **90**, 185001 (2003).
- [20] B. Levitt, Ph.D. thesis, Columbia University, 2004.
- [21] H. Saitoh *et al.*, *Phys. Plasmas* **11**, 3331 (2004).